



**HAL**  
open science

## Adaptive Motion Pooling and Diffusion for Optical Flow

N. V. Kartheek Medathati, Manuela Chessa, Guillaume S. Masson, Pierre Kornprobst, Fabio Solari

► **To cite this version:**

N. V. Kartheek Medathati, Manuela Chessa, Guillaume S. Masson, Pierre Kornprobst, Fabio Solari. Adaptive Motion Pooling and Diffusion for Optical Flow. [Research Report] RR-8695, INRIA Sophia-Antipolis; University of Genoa; INT la Timone; INRIA. 2015. hal-01131099v1

**HAL Id: hal-01131099**

**<https://inria.hal.science/hal-01131099v1>**

Submitted on 12 Mar 2015 (v1), last revised 14 Oct 2015 (v2)

**HAL** is a multi-disciplinary open access archive for the deposit and dissemination of scientific research documents, whether they are published or not. The documents may come from teaching and research institutions in France or abroad, or from public or private research centers.

L'archive ouverte pluridisciplinaire **HAL**, est destinée au dépôt et à la diffusion de documents scientifiques de niveau recherche, publiés ou non, émanant des établissements d'enseignement et de recherche français ou étrangers, des laboratoires publics ou privés.



# Adaptive Motion Pooling and Diffusion for Optical Flow

N. V. Kartheek Medathati, Manuela Chessa, Guillaume S. Masson,  
Pierre Kornprobst, Fabio Solari

**RESEARCH  
REPORT**

**N° 8695**

March 2015

Project-Team Neuromathcomp





## Adaptive Motion Pooling and Diffusion for Optical Flow

N. V. Kartheek Medathati<sup>\*†</sup>, Manuela Chessa<sup>‡</sup>, Guillaume S. Masson<sup>§</sup>, Pierre Kornprobst<sup>†</sup>, Fabio Solari<sup>§</sup>

Project-Team Neuromathcomp

Research Report n° 8695 — March 2015 — 15 pages

**Abstract:** We study the impact of local context of an image (contrast and 2D structure) on spatial motion integration by MT neurons. To do so, we revisited the seminal work by Heeger and Simoncelli (HS) [40] using spatio-temporal filters to estimate optical flow from V1-MT feedforward interactions. However, the HS model cannot deal with several problems encountered in real scenes (e.g., blank wall problem and motion discontinuities). Here, we propose to extend the HS model with adaptive processing by focussing on the role of local context indicative of the local velocity estimates reliability. We set a network structure representative of V1, V2 and MT. We incorporate three functional principles observed in primate visual system: contrast adaptation [38], adaptive afferent pooling [19] and MT diffusion that are adaptive dependent upon the 2D image structure (Adaptive Motion Pooling and Diffusion, AMPD). We evaluated both HS and AMPD models performance on Middlebury optical flow estimation dataset [2]. Our results show that the AMPD model performs better than the HS model and its overall performance is comparable with many modern computer vision. The AMPD model has to be further improved by integrating feedback from MT to V1 to better recover true velocities around motion discontinuities. However, we think that this adaptive model can serve as a ground for future research in biologically-inspired computer vision.

**Key-words:** Bio-inspired approach, optical flow, spatio-temporal filters, motion energy, contrast adaptation, population code, V1, V2, MT, Middlebury dataset

\* Both authors N. V. Kartheek Medathati and Manuela Chessa should be considered as first author.

† INRIA, Neuromathcomp team, Sophia Antipolis, France

‡ University of Genova, DIBRIS, Italy

§ Institut des Neurosciences de la Timone, CNRS, Marseille, France

**RESEARCH CENTRE  
SOPHIA ANTIPOLIS – MÉDITERRANÉE**

2004 route des Lucioles - BP 93  
06902 Sophia Antipolis Cedex

## Intégration et Diffusion Adaptative pour le Calcul du Flot Optique

**Résumé :** Nous étudions l'impact du contexte local d'une image (contraste et structure 2D) sur l'intégration de mouvement spatial par les neurones MT. Pour ce faire, nous avons revisité l'œuvre séminale par Heeger et Simoncelli (HS) [40] utilisant des filtres spatio-temporels et une intégration entre V1 et MT pour estimer le flot optique. Cependant, le modèle HS ne peut pas faire face à plusieurs problèmes rencontrés dans des scènes réelles (par exemple, les problèmes des régions sans contraste et des discontinuités de mouvement). Ici, nous proposons d'étendre le modèle HS avec traitement adaptatif en mettant l'accent sur le rôle du contexte local indicatif de la fiabilité des estimations de vitesse locale. Nous établissons une structure de réseau de neurones représentant les activités dans les aires corticales V1, V2 et MT. Nous intégrons trois principes fonctionnels observés dans le système visuel des primates: l'adaptation au contraste [38], une intégration adaptative [19] et une diffusion adaptative interne à MT qui dépend de la structure 2D de l'image (*Adaptive Motion Pooling and Diffusion*, AMPD). Nous avons évalué les deux modèles HS et AMPD sur la base de test Middlebury [2]. Nos résultats montrent que le modèle AMPD est plus performant que le modèle HS et que sa performance globale est comparable à de nombreuses méthodes de vision par ordinateur. Le modèle AMPD doit encore améliorer en intégrant les interactions descendantes de MT vers V1 afin de mieux récupérer les véritables vitesses au voisinage des discontinuités de mouvement. Cependant nous pensons que ce modèle adaptatif peut servir de référence pour des développements futurs en vision par ordinateur bio-inspiré.

**Mots-clés :** Approche bio-inspirée, flot optique, filtres spatio-temporels, énergie de mouvement, contrat adaptation, codage en population, V1, V2, MT, base de test Middlebury

## Contents

|          |   |           |
|----------|---|-----------|
| <b>1</b> | <b>Introduction</b>                                       | <b>4</b>  |
| <b>2</b> | <b>Biological vision solution</b>                         | <b>4</b>  |
| 2.1      | Cortical hierarchy . . . . .                              | 4         |
| 2.2      | Receptive fields: a local analysis . . . . .              | 5         |
| 2.3      | Contrast adaptive processing . . . . .                    | 6         |
| <b>3</b> | <b>Baseline Model</b>                                     | <b>6</b>  |
| 3.1      | Area V1: Motion Energy . . . . .                          | 7         |
| 3.2      | Area MT: Pattern Cells Response . . . . .                 | 8         |
| 3.3      | Sampling and Decoding: Velocity Estimation . . . . .      | 8         |
| <b>4</b> | <b>Adaptive Motion Pooling and Diffusion Model (AMPD)</b> | <b>9</b>  |
| 4.1      | Area V2: Contrast and Image Structure . . . . .           | 9         |
| 4.2      | Area MT: V2-Modulated Pooling . . . . .                   | 9         |
| 4.3      | MT Lateral Interactions . . . . .                         | 10        |
| <b>5</b> | <b>Results</b>  | <b>11</b> |
| <b>6</b> | <b>Conclusion</b>   | <b>11</b> |

## 1 Introduction

Dense optical flow estimation is a well studied problem in computer vision with several algorithms being proposed and benchmarked over the years [4, 3, 12]. Given that motion information can be used for serving several functional tasks such as navigation, tracking and segmentation, biological systems have evolved sophisticated and highly efficient systems for visual motion information analysis. Understanding the mechanisms adapted by biological systems would be very beneficial for both scientific and technological reasons and has spurred a large number of researchers to investigate underlying neural mechanisms (for reviews see [26, 42, 13, 8, 10]).

Psychophysical and neurophysiological results on global motion integration in primates have inspired many computational models of motion processing. These models first, and still mainly, focus on simulating neural responses to gratings and plaids patterns, are prototypical properties of the local motion estimation stage (area V1) and the motion integration stage (area MT) [25, 45, 40, 36, 44]. However, gratings and plaids are spatially homogeneous motion inputs such that spatial and temporal aspects of motion integration have been largely ignored by these linear-nonlinear filtering models. Dynamical models have been proposed [16, 43, 5] to study these spatial interactions and how they can explain the diffusion of non-ambiguous local motion cues. For instance, [7, 34, 41, 9] have simulated how form-related features in the image such as the luminance gradient or the binocular disparity can play a role in improving motion estimation. However, all these previous models are based on sets of fixed spatiotemporal filters and static nonlinearities. This depart from the highly adaptive and nonlinear properties of visual receptive fields (RFs) [14, 39]. Moreover, these bio-inspired models are barely evaluated in terms of their efficacy on modern computer vision datasets with the notable exceptions such as in [4] (with an early evaluation of spatio-temporal filters) or in [6, 9] (with evaluations on Yosemite or Middlebury videos subset).

In this paper, we propose to fill the gap between studies in biological and computer vision for motion estimation by building our approach on results from visual neuroscience and thoroughly evaluating the method using standard computer vision dataset (Middlebury). The paper is organized as follows. In Sec. 2, we present a brief overview of the motion processing pathway of the primate brain on which our model is based, computational issues to be dealt for the optical flow and known functional principles used by the system to solve them. In Sec. 3, we describe a baseline model for optical flow estimation based on a V1-MT feedforward interactions. This model is largely inspired from Heeger [17, 40]. In Sec. 4 the feedforward model is extended by taking into account both image structure and contrast adaptive pooling and ambiguity resolution through lateral interactions among MT neurons. In order to handle the scale a typical scale-space pyramidal approach has been considered. In Sec. 5 the proposed model is evaluated using the standard Middlebury dataset. In Sec. 6 we conclude by highlighting our main contributions and we relate our work to standard and recent ideas from computer vision.

## 2 Biological vision solution

### 2.1 Cortical hierarchy

In visual neuroscience, properties of low-level motion processing have been extensively investigated in humans [27] and monkeys [28]. Figure 1 illustrates a schematic view of the multiple stages of motion processing in primate cortex. Local motion information is extracted locally through a set of spatiotemporal filters tilling the retinotopic representation of the visual field in area V1. However, these direction-selective cells exhibit several nonlinear properties as the center response is constantly modulated by the surrounding inputs conveyed by feedback and lateral inputs. Direction-selective cells project directly to the motion integration stage. Neurons in the area MT pool these responses over a broad range of spatial and temporal scales, becoming able to extract the direction and speed of a particular surface, regardless its shape or color [10]. Context modulations are not only implemented by center-surround interactions

in areas V1 and MT. For instance, other extra-striate areas such as V2 or V4 project to MT neurons to convey information about the structure of the visual scene, such as the orientation or color of local edges.

## 2.2 Receptive fields: a local analysis

For each neuron in the hierarchy, one can associate a receptive field defined by the region in the visual field that elicits an answer. Receptive fields are first small and become larger going deeper in the hierarchy [28]. The first local analysis of motion is done at the V1 cortical level. The small receptive field size of V1 neurons, and their strong orientation selectivity, poses several difficulties when estimating global motion direction and speed, as illustrated in Fig. 2. In particular, any local motion analyzer will face the three following computational problems [10]:

- Absence of illumination contrast is referred to as blank wall problem in which the local estimator is oblivious to any kind of motion (Fig. 2(b)).
- Presence of luminance contrast changes along only one orientation is often referred to as aperture problem where the local estimator cannot recover the velocity component along the gradient (Fig. 2(c)).
- Presence of multiple motions or multiple objects within the receptive field in which case the local estimator has to be selective to arrive at an accurate estimation (Fig. 2(c)).

In terms of optical flow estimation, feedforward computation involving V1 and MT could be sufficient in the case of regions without any ambiguity. On the contrary, recovering velocity at regions where there is some ambiguity such as aperture or blank wall problems imply to pool reliable information from other, less ambiguous regions in the surrounding. Such spatial diffusion of information is thought to be conveyed by the intricate network of lateral (short-range, or recurrent networks, and long-range) (see [20] for reviews).

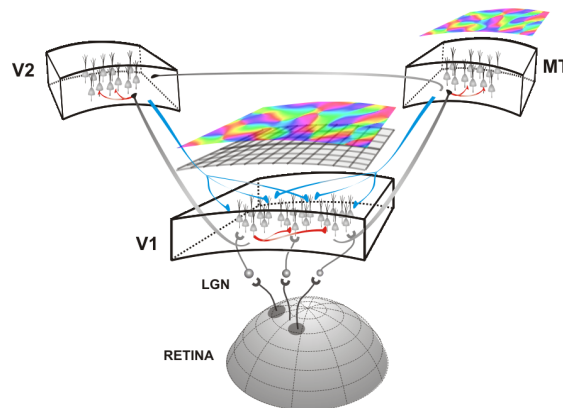


Figure 1: Illustration of the motion processing pathway, with the main cortical areas involved in motion estimation (area V1) and integration (area MT). Interactions with the form pathway are represented by V2 and V4 cortical areas. This cartoon illustrates the variety of connectivities: feedforward (in gray), short- and long-range lateral (in red) and feedback (in blue).

### 2.3 Contrast adaptive processing

The structure of neuronal receptive fields is not static as it has long been thought [14]. Rather, it adapts to the local context of the image so that many of the tuning functions characterizing low-level neurons are in fact dynamical (e.g. [39]). A first series of evidence comes from experiments where the properties of the local inputs change the classical receptive field. For instance orientation-tuning in area V1 and speed tuning of MT neurons are sharper when tested with broad-band texture inputs, as compared to low-dimension gratings (e.g., [15, 32]). Moreover, spatial summation function often broadens as contrast decreases or noise level increases [38]. These observations are complemented by experiments varying the spatial context of this local input. For instance, surround inhibition in V1 and MT neurons becomes stronger at high contrast and center-surround interactions exhibit a large diversity in terms of their relative tunings. Moreover, the spatial structure of these interactions is often more diverse in shape than the classical view of the concentric, Mexican-hat areas (see [10] for a review). Lastly, at each decoding stage, it seems nowadays that tuning functions are weighted by the reliability of the neuronal responses, as varying for instance with contrast or noise levels [23]. Still, these highly adaptive properties have barely been taken into account when modeling visual motion processing. Here, we model some of these mechanisms to highlight their potential impact on optic flow computation. We focus on both the role of local image structure (contrast, texture) and the reliability of these local measurements in controlling the diffusion mechanisms. We investigated how these mechanisms can help solving local ambiguities, and segmenting the flow fields into different surfaces while still preserving the sharpness and precision of natural vision.

## 3 Baseline Model

In this section we revisit the seminal work by Heeger [17, 40] using spatio-temporal filters to estimate optical flow, and propose a baseline model describing V1-MT feedforward interactions. Area V1 comprises simple and complex cells to estimate motion energy [1]. Area MT comprises pattern cells [40, 35]. Then we propose a new decoding stage to obtain a dense optical flow estimation from the MT population response. Note that, although this model is mostly classical, it has never been tested on modern computer vision datasets.

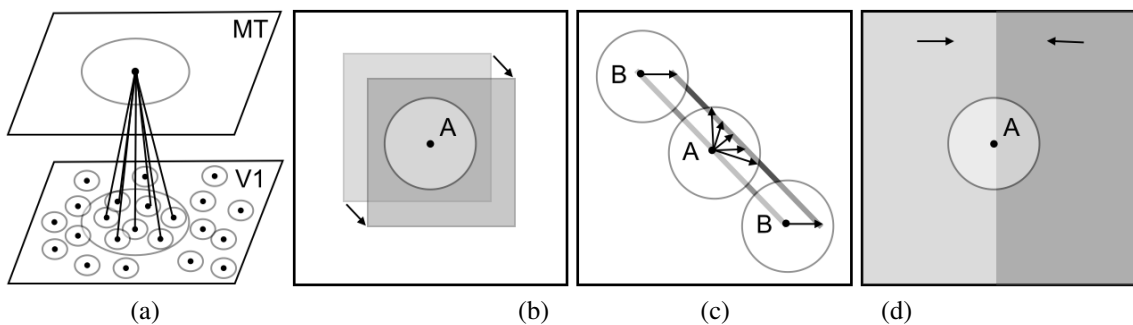


Figure 2: Estimation motion from local observations: (a) Illustration of a pooling step with the corresponding receptive fields; (b) blank wall problem: at position A, the absence of texture gives no information to estimate motion; (c) aperture problem: at position A, only the 1D component of the flow is known; (d) multiple motion: at position A, receptive field integrates different motion informations. Problems in motion estimation.

### 3.1 Area V1: Motion Energy

Let us consider a grayscale image sequence  $I(x, y, t)$ , for all positions  $p = (x, y)$  inside a domain  $\Omega$  and for all time  $t > 0$ . Our goal is to find the optical flow  $v(x, y, t) = (v_x, v_y)(x, y, t)$  defined as the apparent motion at each position  $p$  and time  $t$ .

Simple cells are characterized by the preferred direction  $\theta$  of their contrast sensitivity in the spatial domain and their preferred velocity  $v^c$  in the direction orthogonal to their contrast orientation often referred to as component speed. The RFs of the V1 simple cells are classically modeled using band-pass filters in the spatio-temporal domain. In order to achieve low computational complexity, the spatio-temporal filters are decomposed into separable filters in space and time. Spatial component of the filter is described by Gabor filters  $h$  and temporal component by an exponential decay function  $k$ . Given a spatial size of the receptive field  $\sigma$  and the peak spatial and temporal frequencies  $f_s$  and  $f_t$ , we define the following complex filters by:

$$h(p, \theta, f_s) = B e^{\left(\frac{-(x^2+y^2)}{2\sigma^2}\right)} e^{j2\pi(f_s \cos(\theta)x + f_s \sin(\theta)y)}, \quad (1)$$

$$k(t, f_t) = e^{\left(-\frac{t}{\tau}\right)} e^{j2\pi(f_t t)}, \quad (2)$$

where  $\sigma$  and  $\tau$  are the spatial and temporal scales respectively. Denoting the real and imaginary components of the complex filters  $h$  and  $p$  as  $h_e, k_e$  and  $h_o, k_o$  respectively, and a preferred velocity  $v_c$  related to the frequencies by the relation

$$v^c = \frac{f_t}{f_s}, \quad (3)$$

we introduce the odd and even spatio-temporal filters defined as follows,

$$\begin{aligned} g_o(p, t, \theta, v^c) &= h_o(p, \theta, f_s) k_e(t; f_t) + h_e(p, \theta, f_s) k_o(t; f_t), \\ g_e(p, t, \theta, v^c) &= h_e(p, \theta, f_s) k_e(t; f_t) - h_o(p, \theta, f_s) k_o(t; f_t). \end{aligned}$$

These odd and even symmetric and tilted (in space-time domain) filters characterize V1 simple cells. Using these expressions, we define the response of simple cells, either odd or even, with a preferred direction of contrast sensitivity  $\theta$  in the spatial domain, with a preferred velocity  $v^c$  and with a spatial scale  $\sigma$  by

$$R_{o/e}(p, t, \theta, v^c) = g_{o/e}(p, t, \theta, v^c) \overset{(x,y,t)}{*} I(x, y, t) \quad (4)$$

The complex cells are described as a combination of the quadrature pair of simple cells (4) by using the motion energy formulation,

$$E(p, t, \theta, v^c) = R_o(p, t, \theta, v^c)^2 + R_e(p, t, \theta, v^c)^2,$$

followed by a normalization. Assuming that we consider a finite set of orientations  $\theta = \theta_1 \dots \theta_N$ , to obtain the final V1 response

$$E^{V1}(p, t, \theta, v^c) = \frac{E(p, t, \theta, v^c)}{\sum_{i=1}^N E(p, t, \theta_i, v^c) + \varepsilon}, \quad (5)$$

where  $0 < \varepsilon \ll 1$  is a small constant to avoid divisions by zero in regions with no energies which happen when no spatio-temporal texture is present. The main property of V1 is its tuning to the spatial orientation of the visual stimulus, since the preferred velocity of each cell is related to the direction orthogonal to its spatial orientation.

### 3.2 Area MT: Pattern Cells Response

MT neurons exhibit velocity tuning irrespective of the contrast orientation. This is believed to be achieved by pooling afferent responses in both spatial and orientation domains followed by a non-linearity [40]. The responses of an MT pattern cell tuned to the speed  $v^c$  and to direction of speed  $d$  can be expressed as follows:

$$E^{MT}(p, t; d, v^c) = F \left( \sum_{i=1}^N w_d(\theta_i) \mathcal{P}(E^{V1})(p, t; \theta_i, v^c) \right),$$

where  $w_d$  represents the MT linear weights that give origin to the MT tuning and  $\mathcal{P}(E^{V1})$  corresponds to the spatial pooling.

The physiological evidence suggests that  $w_d$  is a smooth function with central excitation and lateral inhibition. Cosine function shifted over various orientations is a potential function that could satisfy this requirement to produce the responses for a population of MT neurons [24]. Considering the MT linear weights shown in [35],  $w_d(\theta)$  is defined by  $\theta$ :

$$w_d(\theta) = \cos(d - \theta) \quad d \in [0, 2\pi[. \quad (6)$$

This choice allows us to obtain direction tuning curves of pattern cells that behave as in [35].

The spatial pooling term is defined by

$$\mathcal{P}(E^{V1})(p, t; \theta_i, v^c) = \frac{1}{N} \sum_{p'} f_\alpha(\|p - p'\|) E^{V1}(p, t; \theta_i, v^c) \quad (7)$$

where  $f_\mu(s) = \exp(-s^2/2\mu^2)$ ,  $\|\cdot\|$  is the  $L_2$ -norm,  $\alpha$  is a constant,  $\bar{N}$  is a normalization term (here equal to  $2\pi\alpha^2$ ) and  $F(s) = \exp(s)$  is a static nonlinearity chosen as an exponential function [29, 35]. The pooling defined by (7) is a simple spatial Gaussian pooling.

### 3.3 Sampling and Decoding: Velocity Estimation

In order to engineer an algorithm capable of recovering dense optical flow estimates, we still need to address problems of sampling and decoding the population responses of heterogeneously tuned MT neurons.

Indeed, a unique velocity vector cannot be recovered from the activity of a single velocity tuned MT neuron as multiple scenarios could evoke the same activity. However, a unique vector can be recovered from the population activity. In this section, we present a decoding step which was not present in [40, 35] to decode the MT population.

The velocity space could be sampled by considering MT neurons that span over the 2-D velocity space with a preferred set of tuning speed directions in  $[0, 2\pi[$  and also a multiplicity of tuning speeds. Sampling the whole velocity space is not required, as a careful sampling along the cardinal axes could be sufficient to recover the full velocity vector.

In this paper, we sample the velocity space using two MT populations tuned to the directions  $d = 0$  and  $d = \pi/2$  with varying tuning speeds. Here, we adopt a simple weighted sum approach to decode the MT population response [33].

$$\begin{cases} v_x(p, t) = \sum_{i=1}^M v_i^c E^{MT}(p, t, 0, v_i^c), \\ v_y(p, t) = \sum_{i=1}^M v_i^c E^{MT}(p, t, \pi/2, v_i^c). \end{cases} \quad (8)$$

Note that other decoding methods exist such as, e.g. the maximum likelihood estimator [31, 30], however we have adopted the linear weighted sum approach, as a balancing choice between simplicity, computational cost and reliability of the estimates.

## 4 Adaptive Motion Pooling and Diffusion Model (AMPD)

The baseline model involving a feedforward processing from V1 to MT is largely devised to describe physiological and psychophysical observations on motion estimation when the testing stimuli were largely homogeneously textured regions such as moving gratings and plaids. Hence the model is limited in the context of dense flow estimation for natural videos as it has no inherent mechanism to deal with associated sub problems such blank wall problem, aperture problem or occlusion boundaries.

Building on recent results summarized in Sec. 2.3 we model some of these mechanisms to highlight their potential impact on optic flow computation. Considering inputs from area V2, we focus on the role of local context (contrast and image structure) indicative of the reliability of these local measurements in (i) controlling the pooling from V1 to MT and (ii) adding lateral connectivity in MT.

### 4.1 Area V2: Contrast and Image Structure

Our goal is to define a measure of contrast which is indicative of the aperture and blank wall problems using the responses of spatial Gabor filters. There exist several approaches to characterize the spatial content of an image from Gabor filter. For example, in [21] the authors propose the phase congruency approach which detects edges and corners irrespectively of contrast in an image. In dense optical flow estimation problem, region with texture are less likely to suffer blank wall and aperture problems even though edges are susceptible to aperture problem. So phase congruency approach cannot be used directly and we propose the following simple alternative approach.

Let  $h_{\theta_i}$  the Gabor filter for edge orientation  $\theta_i$ , we define

$$R(p) = (R_{\theta_1}(p), \dots, R_{\theta_N}(p)) \text{ where } R_{\theta_i}(p) = |h_{\theta_i} * I|(p).$$

Given an edge orientation at  $\theta_i$ ,  $R_{\theta_i}$  is maximal when crossing the edge and  $\nabla R_{\theta_i}$  indicate the direction to go away from edge.

Then the following contrast/cornerness measure is proposed as follows, taking into consideration the amount of contrast at a given location and also ensuring that contrast is not limited to a single orientation giving raise to aperture problem.

$$\mu(R)(p) = \frac{1}{N} \sum_i R_{\theta_i}(p), \quad (9)$$

$$C(p) = H_{\xi}(\mu(R(p)))(1 - \sigma^2(R(p))/\sigma_{max}^2), \quad (10)$$

where  $\mu(R(p))$  (resp.  $\sigma^2(R(p))$ ) denote the average (resp. variance) of components of  $R$  at position  $p$ ,  $H_{\xi}(s)$  is a step function ( $H_{\xi}(s) = 0$  if  $s \leq \xi$  and 1 otherwise) and  $\sigma_{max}^2 = \max_{p'} \sigma^2(R(p))$ . The term  $H_{\xi}(\mu(R(p)))$  is an indicator of contrast as it measures the Gabor energies: in regions with strong contrast or strong texture in any orientation this term equals to one; in a blank wall situation, it is equal to zero. The term  $(1 - \sigma^2(R(p))/\sigma_{max}^2)$  measures how strongly the contrast is oriented in a single direction: it is higher when there is only contrast in one direction and lower when there is contrast in more than one orientation (thus it is an indicator of where there is aperture problem).

### 4.2 Area MT: V2-Modulated Pooling

Most of the models currently pool V1-afferents using a linear fixed receptive field size, which does not adapt itself to the local gradient or respect discontinuities in spatio-temporal reposes. This might lead to degradation in the velocity estimates by blurring edges/kinetic boundaries. Thus it is advantageous to make the V1 to MT pooling adaptive as a function of texture edges.

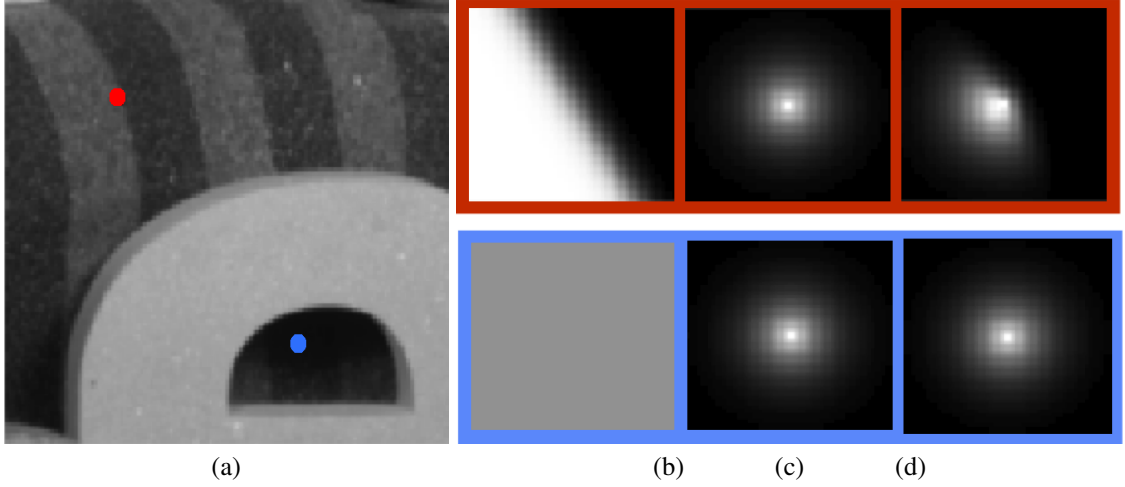


Figure 3: Impact of local contrast on pooling strategy: (a) Sample input indicating two different locations being sampled. (b) (A) Anisotropy term, (B) Spatial term, (C) Pooling region.

We propose to modify the pooling stage as follows

$$E^{MT}(p, t; d, v^c) = F \left( \sum_{i=1}^N w_d(\theta_i) \tilde{\mathcal{P}}(E^{V1})(p, t; \theta_i, v^c) \right),$$

where the spatial pooling become functions of image structure. We propose the following texture-dependent spatial pooling:

$$\begin{aligned} \mathcal{P}(E^{V1})(p, t; \theta_i, v^c) = \\ \frac{1}{\bar{N}(p, \theta_i)} \sum_{p'} f_{\alpha(\|R\|(p))}(\|p - p'\|) g_i(p, p') E^{V1}(p, t; \theta_i, v^c) \end{aligned} \quad (11)$$

where  $\bar{N}(p, \theta_i) = \sum_{p'} f_{\alpha(\|R\|(p))}(\|p - p'\|) g_i(p, p')$  is a normalizing term. The two weights are now depending on image structure. The variance of the distance term  $\alpha$ , i.e., the size of the integration domain, now depends on the structure  $R_{\theta_i}$  as follows

$$\alpha(\|R\|(p)) = \alpha_{max} e^{-\eta \frac{\|R\|^2(p)}{r_{max}}}, \quad (12)$$

where  $\eta$  is a constant,  $r_{max} = \max_{p'} \{\|R\|^2(p')\}$ . Then there is an additional term  $g_i(p, p')$  to enable anisotropic pooling close to image structures so that discontinuities could be better preserved. Here we propose to define  $g_i$  by

$$g_i(p, p') = S_{\lambda, \nu} \left( -\frac{\nabla R_{\theta_i}(p)}{\|\nabla R_{\theta_i}\| + \varepsilon} \cdot (p' - p) \right), \quad (13)$$

where  $S_{\lambda, \nu} = 1/(1 + \exp(-\lambda(x - \nu)))$  is a sigmoid function and  $\varepsilon$  a small constant. Note that this term is used only in regions where  $\|\nabla R_{\theta_i}\|$  is greater than a threshold. Fig. 3(a) gives examples of the pooling coefficients at different  $p$  locations.

### 4.3 MT Lateral Interactions

We model the lateral iterations for the velocity information spread (from the regions where there is less ambiguity to regions with high ambiguity, see Sec. 2.2) whilst preserving discontinuities in motion and

illumination. To do so, we propose an iterated trilateral filtering defined by:

$$u^{n+1}(p) = \frac{1}{N(p)} \sum_{p'} W(p, p') u^n(p'), \quad (14)$$

$$c^{n+1}(p) = c^n(p) + \lambda \left( \max_{p' \in \mathcal{N}(p)} c^n(p') - c^n(p) \right) \quad (15)$$

$$u^0(p) = E^{MT}(p, t; \theta_i, v^c), \quad (16)$$

$$c^0(p) = C(p), \quad (17)$$

where

$$W(p, p') = c^n(p') f_\alpha(\|p - p'\|) f_\beta(c^n(p)(u^n(p') - u^n(p))) f_\gamma(I(p') - I(p)) u^n(p'), \quad (18)$$

and  $\mathcal{N}(p)$  is a local neighborhood around  $p$ . The term  $c(p')$  ensures that more weight is given naturally to high confidence estimates; The term  $c(p)$  inside  $f_\beta$  ensures that differences in the MT responses are ignored when confidence is low facilitating the diffusion of information from regions with high confidence and at the same time preserves motion discontinuities or blurring at the regions with high confidence.

## 5 Results

In order to test the method a multi-scale version of both the baseline approach and approach with adaptive pooling are considered. The method is applied on a Gaussian pyramid with 6 scales, the maximum number of scales that could be reliably used for the spatio-temporal filter support that has been chosen.

A first test was done on Yosemite sequence as it is widely used in both computer vision and biological vision studies (see Fig. 4, first row). For the baseline model, AAE=3.55 ± 2.92 and for AMPD we have AAE=3.00 ± 2.21. This can be compared to what has been obtained with previous biologically-inspired models such as the original Heeger approach (AAE=11.74°, but estimated 44.8% of the most reliable regions, see [4]) and the neural model from Bayerl and Neumann (AAE=6.20°, [5]), showing an improvement. One can do comparisons with standard computer vision approaches such as Pyramidal Lucas and Kanade (AAE=6.41°) and Horn and Schunk (AAE=6.41°, [18]), showing comparable performance.

The results on the Middlebury training set show improvements of the proposed method with respect to the baseline (see Table 1). For qualitative comparison, sample results are also presented in Fig. 4. The relative performance of extended method can be understood by observing  $\delta$ AAE, difference between the baseline AAE map and the AAE map of AMPD which are presented in Figure 4 (last column): the improvements are prominent at the edges, e.g. see the  $\delta$ AAE column for the RubberWhale and Urban2 sequence.

## 6 Conclusion

In this paper, we have proposed a new algorithm that incorporates three functional principles observed in primate visual system, namely contrast adaptation, image structure based afferent pooling and ambiguity based lateral interaction. This is an extension to an earlier algorithm developed by Heeger et al. [17, 40] which is appreciated by both computer vision and biological vision communities.

Contemporary computer vision methods to [17] such as [22] and [18] which study local motion estimation and global constraints to solve aperture problem have been revisited by the computer vision with great interest [11] and a lot of investigations are being carried out to regulate the information diffusion

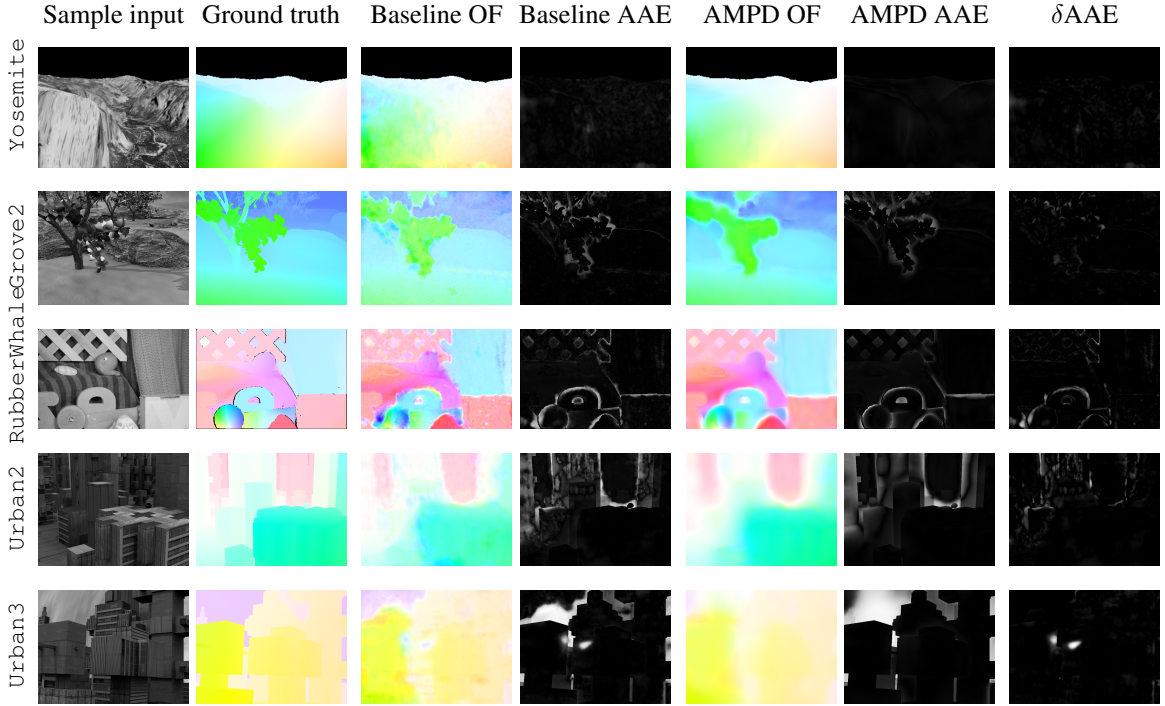


Figure 4: Sample results on Yosemite sequence and a subset of Middlebury training set.  $\delta AAE = AAE_{Baseline} - AAE_{AMPD}$

| Sequence    | Baseline          |                 | AMPD              |                 |
|-------------|-------------------|-----------------|-------------------|-----------------|
|             | AAE $\pm$ STD     | EPE $\pm$ STD   | AAE $\pm$ STD     | EPE $\pm$ STD   |
| grove2      | 4.28 $\pm$ 10.25  | 0.29 $\pm$ 0.62 | 4.07 $\pm$ 9.29   | 0.27 $\pm$ 0.56 |
| grove3      | 9.72 $\pm$ 19.34  | 1.13 $\pm$ 1.85 | 10.66 $\pm$ 19.25 | 1.11 $\pm$ 1.61 |
| Hydrangea   | 5.96 $\pm$ 11.17  | 0.62 $\pm$ 0.96 | 5.48 $\pm$ 11.10  | 0.50 $\pm$ 0.69 |
| RubberWhale | 10.20 $\pm$ 17.67 | 0.34 $\pm$ 0.54 | 8.87 $\pm$ 13.16  | 0.30 $\pm$ 0.42 |
| urban2      | 14.51 $\pm$ 21.02 | 1.46 $\pm$ 2.13 | 12.70 $\pm$ 19.92 | 1.09 $\pm$ 1.31 |
| urban3      | 15.11 $\pm$ 35.28 | 1.88 $\pm$ 3.27 | 12.78 $\pm$ 31.36 | 1.32 $\pm$ 2.25 |

Table 1: Error measurements on Middlebury training set

from non-ambiguous regions to ambiguous regions based on image structure (see, e.g., [37]). Very few attempts have been made to incorporate these ideas into spatio-temporal filter based models such as [17]. Given the recent growth in neuroscience, it is very interesting to revisit this model incorporating the new findings and examining the efficacy.

This paper provides a baseline for future research in biologically-inspired computer vision, considering that functional principles uncovered in biological vision are a rich source of ideas for future developments. This study is the first to rigorously evaluate V1-MT feedforward model on modern computer vision dataset such as Middlebury, together with the improvements described in this paper. The extended improves the flow estimation compared to Heeger et. al. and has a great potential to be further improved by incorporating machine learning techniques. It has opened up several interesting sub problems, which could be of relevance to biologists as well, for example what could be afferent pooling strategy of MT

when there are multiple surfaces or occlusion boundaries within the MT receptive field? Can a better dense optical flow map be recovered by considering decoding problem as a debarring problem due the spatial support of the filters etc.

This work could act as a good starting point for building scalable computer vision algorithms for motion processing that are rooted in biology. For that reason we propose to share the code in order to encourage research in this direction.<sup>1</sup>

## Acknowledgments

The research leading to these results has received funding from the European Union’s Seventh Framework Programme (FP7/2007-2013) under grant agreement no. 318723 (MATHEMACS) and grant agreement no. 269921 (BrainScaleS).

## References

- [1] E.H. Adelson and J.R. Bergen. Spatiotemporal energy models for the perception of motion. *Journal of the Optical Society of America A*, 2:284–299, 1985. [6](#)
- [2] S Baker, D Scharstein, J P Lewis, S Roth, M J Black, and R Szeliski. A database and evaluation methodology for optical flow. *International Journal of Computer Vision*, 92(1):1–31, 2011. [1](#), [2](#)
- [3] S. Baker, D. Scharstein, JP Lewis, S. Roth, M.J. Black, and R. Szeliski. A database and evaluation methodology for optical flow. In *International Conference on Computer Vision, ICCV’07*, pages 1–8, 2007. [4](#)
- [4] J.L. Barron, D.J. Fleet, and S.S. Beauchemin. Performance of optical flow techniques. *The International Journal of Computer Vision*, 12(1):43–77, 1994. [4](#), [11](#)
- [5] P. Bayerl and H. Neumann. Disambiguating visual motion through contextual feedback modulation. *Neural Computation*, 16(10):2041–2066, 2004. [4](#), [11](#)
- [6] P. Bayerl and H. Neumann. A fast biologically inspired algorithm for recurrent motion estimation. *Pattern Analysis and Machine Intelligence, IEEE Transactions on*, 29(2):246–260, 2007. [4](#)
- [7] C. Beck and H. Neumann. Interactions of motion and form in visual cortex – a neural model. *Journal of Physiology - Paris*, 104:61–70, 2010. [4](#)
- [8] R.T. Born and D.C. Bradley. Structure and function of visual area MT. *Annu. Rev. Neurosci*, 28:157–189, 2005. [4](#)
- [9] J.D. Bouecke, Emilien Tlapale, Pierre Kornprobst, and H. Neumann. Neural mechanisms of motion detection, integration, and segregation: From biology to artificial image processing systems. *EURASIP Journal on Advances in Signal Processing*, 2011, 2011. special issue on Biologically inspired signal processing: Analysis, algorithms, and applications. [4](#)
- [10] D.C. Bradley and M.S. Goyal. Velocity computation in the primate visual system. *Nature Reviews Neuroscience*, 9(9):686–695, 2008. [4](#), [5](#), [6](#)

---

<sup>1</sup>The link will be provided, upon completion of review process.

- [11] Andrés Bruhn, Joachim Weickert, and Christoph Schnörr. Lucas/kanade meets horn/schunck: Combining local and global optic flow methods. *International Journal of Computer Vision*, 61:211–231, 2005. 11
- [12] Daniel J. Butler, Jonas Wulff, Garrett B. Stanley, and Michael J. Black. A naturalistic open source movie for optical flow evaluation. In *Proceedings of the 12th European Conference on Computer Vision - Volume Part VI, ECCV'12*, pages 611–625, Berlin, Heidelberg, 2012. Springer-Verlag. 4
- [13] C.W.G Clifford and M.R Ibbotson. Fundamental mechanisms of visual motion detection: models, cells and functions. *Progress in Neurobiology*, 68(6):409 – 437, 2002. 4
- [14] A. Fairhall. The receptive field is dead. long life the receptive field? *Current Opinion in Neurobiology*, 25:9–12, 2014. 4, 6
- [15] Jeremy Freeman, Cosey M Ziemba, David J Heeger, Eero P Simoncelli, and J Anthony Movshon. A functional and perceptual signature of the second visual area in primates. *Nature Neuroscience*, 16:974–981, 2013. 6
- [16] S. Grossberg and E. Mingolla. Neural dynamics of form perception: boundary completion, illusory figures, and neon color spreading. *Psychological review*, 92(2):173–211, 1985. 4
- [17] D.J. Heeger. Optical flow using spatiotemporal filters. *The International Journal of Computer Vision*, 1(4):279–302, January 1988. 4, 6, 11, 12
- [18] B.K. Horn and B.G. Schunck. Determining Optical Flow. *Artificial Intelligence*, 17:185–203, 1981. 11
- [19] X. Huang, T.D. Albright, and G.R. Stoner. Adaptive surround modulation in cortical area MT. *Neuron*, 53:761–770, 2007. 1, 2
- [20] U.J. Ilg and G.S. Masson. *Dynamics of Visual Motion Processing: Neuronal, Behavioral, and Computational Approaches*. SpringerLink: Springer e-Books. Springer Verlag, 2010. 5
- [21] Peter Kovesi. Image features from phase congruency. *Videre: A Journal of Computer Vision Research*. MIT Press, 1(3), 1999. 9
- [22] B. Lucas and T. Kanade. An iterative image registration technique with an application to stereo vision. In *International Joint Conference on Artificial Intelligence*, pages 674–679, 1981. 11
- [23] Wei Ji Ma and Mehrdad Jazayeri. Neural coding of uncertainty and probability. *Annual Review of Neuroscience*, 37(1):205–220, 2014. 6
- [24] J. H. Maunsell and D. C. Van Essen. Functional properties of neurons in middle temporal visual area of the macaque monkey. I. selectivity for stimulus direction, speed, and orientation. *Journal of Neurophysiology*, 49(5):1127–1147, 1983. 8
- [25] J.A. Movshon, E.H. Adelson, M.S. Gizzi, and W.T. Newsome. The analysis of visual moving patterns. *Pattern recognition mechanisms*, pages 117–151, 1985. 4
- [26] Ken Nakayama. Biological image motion processing: A review. *Vision Research*, 25:625–660, 1984. 4
- [27] S. Nishida. Advancement of motion psychophysics: Review 2001-2010. *Journal of Vision*, 11(5):11, 1–53, 2011. 4

- [28] Guy A. Orban. Higher order visual processing in macaque extrastriate cortex. *Physiological Reviews*, 88(1):59–89, 2008. 4, 5
- [29] Liam Paninski. Maximum likelihood estimation of cascade point-process neural encoding models. *Network: Computation in Neural Systems*, 15(4):243–262, 2004. 8
- [30] A. Pouget, P. Dayan, and R. Zemel. Information processing with population codes. *Nature Reviews Neuroscience*, 1(2):125–132, 2000. 8
- [31] A. Pouget, K. Zhang, S. Deneve, and P. E. Latham. Statistically efficient estimation using population coding. *Neural Computation*, 10(2):373–401, 1998. 8
- [32] Nicholas Priebe, Carlos Cassanello, and Stephen Lisberger. The neural representation of speed in macaque area MT/V5. *Journal of Neuroscience*, 23(13):5650–5661, July 2003. 6
- [33] Kamiar Rahnama Rad and Liam Paninski. Information rates and optimal decoding in large neural populations. In John Shawe-Taylor, Richard S. Zemel, Peter L. Bartlett, Fernando C. N. Pereira, and Kilian Q. Weinberger, editors, *NIPS*, pages 846–854, 2011. 8
- [34] F. Raudies and H. Neumann. A model of neural mechanisms in monocular transparent motion perception. *Journal of Physiology-Paris*, 104(1-2):71–83, 2010. 4
- [35] N C Rust, V Mante, E P Simoncelli, and J A Movshon. How MT cells analyze the motion of visual patterns. *Nature Neuroscience*, 9(11):1421–1431, 2006. 6, 8
- [36] N.C. Rust, V. Mante, E.P. Simoncelli, and J.A. Movshon. How MT cells analyze the motion of visual patterns. *Nature Neuroscience*, 9:1421–1431, 2006. 4
- [37] J. Sánchez, A. Salgado, and N. Monzón. Preserving accurate motion contours with reliable parameter selection. In *ICIP*, pages 209–213, 2014. 12
- [38] Michael P. Sceniak, Dario L. Ringach, Michael J. Hawken, and Robert Shapley. Contrast’s effect on spatial summation by macaque V1 neurons. *Nature Neuroscience*, 2(8):733–739, August 1999. 1, 2, 6
- [39] T.O. Sharpee, H. Sugihara, A.V. Kurgansky, S.P. Rebrik, M.P. Stryker, and K.D. Miller. Adaptive filtering enhances information transmission in visual cortex. *Nature*, 439:936–942, 2006. 4, 6
- [40] E.P. Simoncelli and D.J. Heeger. A model of neuronal responses in visual area MT. *Vision Research*, 38:743–761, 1998. 1, 2, 4, 6, 8, 11
- [41] Emilien Tlapale, Guillaume S. Masson, and Pierre Kornprobst. Modelling the dynamics of motion integration with a new luminance-gated diffusion mechanism. *Vision Research*, 50(17):1676–1692, August 2010. 4
- [42] D. C. Van Essen and J. L. Gallant. Neural mechanisms of form and motion processing in the primate visual system. *Neuron*, 13:1–10, July 1994. 4
- [43] Y. Weiss and E. H. Adelson. Slow and smooth: A Bayesian theory for the combination of local motion signals in human vision. *Center for Biological and Computational Learning Paper*, 1998. 4
- [44] Y. Weiss and E.H. Adelson. Adventures with gelatinous ellipses – constraints on models of human motion analysis. *Perception*, 29:543–566, 2000. 4
- [45] H.R. Wilson, V.P. Ferrera, and C. Yo. A psychophysically motivated model for two-dimensional motion perception. *Visual Neuroscience*, 9(1):79–97, July 1992. 4



**RESEARCH CENTRE  
SOPHIA ANTIPOLIS – MÉDITERRANÉE**

2004 route des Lucioles - BP 93  
06902 Sophia Antipolis Cedex

Publisher  
Inria  
Domaine de Voluceau - Rocquencourt  
BP 105 - 78153 Le Chesnay Cedex  
[inria.fr](http://inria.fr)

ISSN 0249-6399